nature portfolio

https://doi.org/10.1038/s41586-025-09174-w

Supplementary information

Silicate clouds and a circumplanetary disk in the YSES-1 exoplanet system

In the format provided by the authors and unedited

Silicate index measurements

To analyze the silicate absorption in YSES-1 c, we fit the data using ForMoSA with the cloud-free atmospheric model ATMO[1] to estimate the pseudo-continuum as the silicate absorption at 10 µm should not be present. The pseudo-continuum is subtracted from the data, and the residuals are integrated to obtain a spectral index. We estimated this silicate index for YSES-1 c and for objects of a mid-resolution (R ≈ 90) spectral library obtained with Spitzer/IRS. This sample includes young and old (< 10 Myr to > 1 Gyr) cold, isolated, and low mass brown dwarfs (late-M to T types).

We compare YSES-1 c to three objects: VHS 1256 b observed with JWST/MIRI[2], and 2MASS 2148 and 2MASS 0355. 2MASS 2148 was chosen due to having deep absorption and a high index, and 2MASS 0355 was chosen due to having iron-rich silicate clouds[3]. We defined two spectral windows on both sides of the feature between [6.0, 8.0] and [12.0, 14.0] µm. For YSES-1 c, the left window was [7.0, 8.5] µm to avoid being biased by the redshifted feature. Figure 2 (center) shows that the silicate absorption is shifted ~0.5 µm to the red. The origin of this morphological variation is explored in "Silicate Feature Cloud Modeling" in the Methods section. To calculate the spectral index, we integrated this relative deviation between [8, 11.5] µm. Although it has a similar index to VHS 1256 b, Figure 2 (center) shows a difference in the morphology of the silicate absorption.

Host Star Measurements

We used a high-resolution UVES/VLT spectrum (R = 107,000; Program: 106.20ZM.00)[4] spanning 480-680 nm with a signal-to-noise ratio (SNR) per pixel of 97. To determine effective temperature (T_{eff}), we calibrated photometric points using Gaia (G, BP, RP) and 2MASS (J, H, K) magnitudes[5]. We calculated the surface gravity (log g) using bolometric corrections, the photometric effective temperature, the mass (1.1 M_{Sun}) and E(B-V)=0[6,7].

Microturbulence velocity (V_t) was obtained using the photometric T_{eff} and log g[8]. The resulting atmospheric parameters were T_{eff} = 4680 ± 53 K, log g = 4.62 ± 0.05 dex, and V_t = 0.75±0.10 km/s with the errors calculated via monte carlo. We fit the iron lines (TSFitPy[104]) with a linelist of 35 Fe I lines and 17 Fe II lines[9]. We assumed solar chemical composition[10]. T_{eff} and log g were determined from the excitation and ionization balance, while V_t was optimized by imposing no correlation between the reduced equivalent widths of the spectral lines (log(EW/lambda) and their corresponding abundances.

The final parameters closely matched the photometric ones, resulting in T_{eff} = 4680 ± 70 K, log g = 4.60 ± 0.10 dex, and V_t = 0.90 ± 0.10 km/s. The metallicity was [Fe/H] = -0.01 ± 0.05. We derived [Si/Fe] = -0.04 ± 0.10 and [Ca/Fe] = 0.00 ± 0.05, indicating a solar-scaled alpha-element abundance pattern. We also confirmed the significant overabundance of the s-process element barium with [Ba/Fe] = +0.43 ± 0.12 dex[11]. We determined carbon abundances by synthesizing the C_2 Swan bands at 5628/5636 and 5160/5166 Angstroms and found [C/Fe] = 0.01 ± 0.05 dex

(A(C)=8.43; see Extended Figure 7). To estimate oxygen abundances, we used XShooter spectra (R~17,000, Program: 103.2008.001). We applied NLTE corrections and obtained [O/H] = -0.02 ± 0.07 (A(O) = 8.67)[12]. We found a stellar (C/O) ratio of 0.575±0.10, consistent with that of the Sun[10].

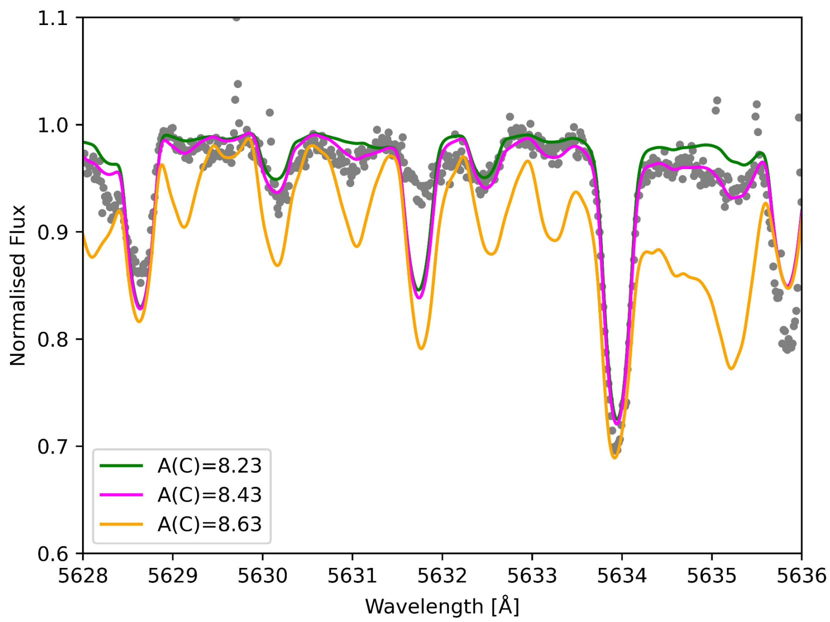

Supplemental Methods Figure 1: C_2 Swan bands at 5628/5636 and 5160/5166 Angstroms in UVES spectra of Solar-type host star YSES-1. Comparison of the observed (dotted gray) and synthetic spectra around the C_2 Swan band at 5630 Å. The three solid lines indicate the best-fit carbon abundance (A(C) = 8.43) with an uncertainty of ±0.2 dex.

[1] Tremblin, P., Chabrier, G., Baraffe, I., Liu, M. C., Magnier, E., et al. Cloudless Atmospheres for Young Low-gravity Substellar Objects. The Astrophysical Journal, 850, 46 (2017)

[2] Miles, B. E., Biller, B. A., Patapis, P., Worthen, K., Rickman, E., et al. The JWST Early-release Science Program for Direct Observations of Exoplanetary Systems II: A 1 to 20 μm Spectrum of the Planetary-mass Companion VHS 1256-1257 b. The Astrophysical Journal Letters, 946, L6 (2023)

[3] Suárez, G., Vos, J. M., Metchev, S., Faherty, J. K., Cruz, K., et al. Ultracool Dwarfs Observed with the Spitzer Infrared Spectrograph: Equatorial Latitudes in L Dwarf Atmospheres Are Cloudier. The Astrophysical Journal Letters, 954, L6 (2023)

[4] Dekker, H., D'Odorico, S., Kaufer, A., Delabre, B., Kotzlowski, H., et al. Design, construction, and performance of UVES, the echelle spectrograph for the UT2 Kueyen Telescope at the ESO Paranal Observatory. Optical and IR Telescope Instrumentation and Detectors, 4008, 534-545 (2000)

[5] Casagrande, L., Lin, J., Rains, A. D., Liu, F., Buder, S., et al. The GALAH survey: effective temperature calibration from the InfraRed Flux Method in the Gaia system. Monthly Notices of the Royal Astronomical Society, 507, 2684-2696 (2021)

[6] Casagrande, L., VandenBerg, D. A., On the use of Gaia magnitudes and new tables of bolometric corrections. Monthly Notices of the Royal Astronomical Society, 479, L102-L107 (2018)

[7] Pecaut, M. J., Mamajek, E. E., The star formation history and accretion-disc fraction among the K-type members of the Scorpius-Centaurus OB association. Monthly Notices of the Royal Astronomical Society, 461, 794-815 (2016)

[8] Dutra-Ferreira, L., Pasquini, L., Smiljanic, R., Porto de Mello, G., Steffen, M., et al. Consistent metallicity scale for cool dwarfs and giants. A benchmark test using the Hyades. Astronomy & Astrophysics, 585, A75 (2016)

[9] Gerber, J. M., Magg, E., Plez, B., Bergemann, M., Heiter, U., et al. Non-LTE radiative transfer with Turbospectrum. Astronomy & Astrophysics, 669, A43 (2023)

[10] Asplund, M., Grevesse, N., Sauval, A. J., Scott, P., The Chemical Composition of the Sun. Annual Review of Astronomy and Astrophysics, 47, 481-522 (2009)

[11] Heiter, U., Lind, K., Bergemann, M., Asplund, M., Mikolaitis, Š., et al. Atomic data for the Gaia-ESO Survey. Astronomy & Astrophysics, 645, A106 (2021)

[12] D'Orazi, V., Baratella, M., Lugaro, M., Magrini, L., Pignatari, M., et al. The Complex Behaviour of s-Process Element Abundances at Young Ages. Universe, 8, 110 (2022)